

Numerical and Experimental Analysis of an Industrial Spark Arrester Applied to Fire Prevention in Grain Dryers

Bruno Stanke, Rou-Yi Pan, Jonathan Utzig, Henry França Meier, Rodrigo Koerich Decker

University of Blumenau, Department of Chemical Engineering, Sao Paulo St, 3250, Blumenau, Brazil, 89030-000

Abstract: Cyclonic spark arresters are low-pressure-drop filtration devices used to separate sparks generated from biomass combustion in grain dryers, contributing to fire prevention in the agricultural sector. In this study, the CFD code CYCLO-EE5, specifically developed for cyclone simulations, was applied to analyze a full-scale industrial case. Numerical results revealed that following abrupt pressure variations within the equipment, accumulated particulate matter is intermittently released via discharge and/or entrainment events. This phenomenon may be associated with failures in retaining potentially incendiary sparks, thereby increasing operational risks. To verify this behavior, experimental field measurements of pressure drop were performed under the same operating conditions used as reference for the numerical analysis. The integrated results indicated intermittent accumulation and discharge, providing novel insights to improve fire prevention systems in agricultural dryers.

Keywords: Spark arresters; Cyclone; Computational Fluid Dynamics.

1. Introduction

Brazil, as one of the world's leading grain producers and exporters, is expected to see a 16% growth in the 2024/2025 harvest compared to the previous cycle, according to estimates by the National Supply Company (CONAB, 2025). While economically positive, this increase in production heightens challenges related to operational safety and the sustainability of the production chain. Among the critical points is the drying stage, which is essential for ensuring grain quality and preservation but also poses a high risk of fires and explosions, particularly when biomass combustion is used as an energy source (Zarpellon, 2025).

National and international studies have demonstrated that dust explosions in agro-industrial facilities remain recurring, high-impact events that can cause significant human, material, and environmental losses (Eckhoff & Li, 2021; Tian et al., 2025). In the Brazilian context, beyond the direct implications for occupational safety, such events jeopardize the competitiveness of agribusiness, which accounts for a significant portion of the national GDP (Gross Domestic Product). Thus, strategies to prevent spark ignition and reduce the emission of particles with incendiary potential are fundamental to the sustainability and continuity of operations.

From a scientific perspective, the risk of dust ignition is associated with factors such as particle size and distribution, cloud concentration, turbulence, humidity, and oxygen availability (Khudhur et al., 2021; Tian et al., 2025). Recent research has focused on developing numerical models to estimate the minimum ignition energy (MIE) that accounts for realistic particle size distributions, enabling more robust and conservative predictions for risk assessment (Chen et al., 2022). Other lines of investigation address suppression strategies, such as the use of inert gases (CO₂ and N₂), which have proven effective in reducing the intensity and propagation speed of flames in biomass dust (Huang et al., 2022).

Despite these advances, industrial reports indicate that failures in particle collection and retention systems still rank among the primary causes of fires and secondary explosions, which are often more severe than primary ones (Eckhoff & Li, 2021). In these situations, accumulated dust layers or uncaptured sparks act as triggers, enhancing the risk of large-magnitude events. This reinforces the importance of robust technologies for solid particle separation in industrial processes.

Among these technologies, cyclonic equipment stands out as a widely used solution for separating solid particles in gas-solid flows through centrifugal force. Unlike conventional high-efficiency cyclones, spark arresters are designed with distinct geometric proportions to operate at considerably lower pressure drops while retaining larger, incandescent

biomass particles before the hot gas stream enters the grain dryers (Hoffmann & Stein, 2008). Typical separation efficiencies for standard cyclones range from 90% to 99%, whereas spark arresters often operate with significantly lower baseline efficiencies, which can fluctuate dynamically. Industrial safety standards for agricultural facilities and deflagration venting, such as those prescribed by NFPA 68, highlight the critical need to manage uncaptured sparks to prevent subsequent dust cloud ignitions (Tascon et al., 2016). The accumulation of these particles, along with impurities such as comcobs and husks, creates a highly susceptible environment for smoldering combustion and fires (Zarpellon, 2025).

Historically, the performance prediction of cyclonic devices has relied on classical semi-empirical models, such as those proposed by Lapple and Muschelknautz, which provide reasonable estimates for average collection efficiency under steady-state conditions (Sgrott et al., 2015). However, these foundational models lack the capacity to account for the highly transient fluid dynamic phenomena occurring within the equipment. Recent investigations have demonstrated that actual performance is strongly influenced by dynamic flow instabilities, including pressure-drop fluctuations, localized vortex breakdowns, and particle dispersion patterns in turbulent flow (Zhao & Ambrose, 2019; Zhao & Ambrose, 2022). Furthermore, studies focusing on multiphase interactions reveal that large particles can act as flow obstacles, altering dust dispersibility and promoting phenomena such as particle re-entrainment and saltation (Zhang et al., 2024). In cyclonic spark arresters, these flow instabilities can trigger intermittent cycles of solid accumulation and sudden discharge, a highly transient phenomenon herein termed the "avalanche effect", which drastically elevates explosion risks and alters flame propagation characteristics if ignited (Ding et al., 2024; Sulaiman et al., 2024).

In this scenario, advances in Computational Fluid Dynamics (CFD) represent a robust alternative to overcoming the limitations of traditional empirical models. Dedicated multi-phase codes, such as CYCLO-EE5, enable high-fidelity simulations at an industrial scale, accounting for complex solid-solid and gas-solid interactions through an Eulerian-Eulerian approach (Meier et al., 2011; Costa et al., 2013; Sgrott et al., 2015). To address these transient phenomena, this study aims to evaluate the fluid-dynamic behavior of a full-scale industrial cyclonic spark arrester through an integrated numerical and experimental analysis of differential-pressure measurements and multiphase simulations. By characterizing the relationships among oscillatory pressure processes, separation efficiency, and the emission of potentially incendiary particles,

*Corresponding author: Rodrigo Koerich Decker. E-mail: rkdecker@furb.br

Received 13 May 2026; Received in revised form 24 May 2026; Accepted 25 June 2026; Published: 4 July 2026.

Copyright: © 2026 The Author(s). Published by Engineering & Sustainability Journal (ESJ). This is an open-access article distributed under the terms and conditions of the Creative Commons Attribution 4.0 International License (<https://creativecommons.org/licenses/by/4.0/>).

this research makes a novel contribution to industrial process safety and to engineering solutions for risk mitigation in biomass-energy agricultural systems. The original value of this work lies in the quantitative and phenomenological demonstration of intermittent particle accumulation and discharge, the avalanche effect, and the proof that equipment reliability and sustainable fire prevention in agro-industrial facilities cannot be adequately predicted or ensured by conventional steady-state design models alone.

2. Materials And Methods

2.1. Numerical Modeling and Cyclo-Ee5 Code

The numerical simulations were performed using the CYCLO-EE5 code, a dedicated 3D-axisymmetric Computational Fluid Dynamics (CFD) tool developed specifically for cyclonic separation devices. The code solves the governing conservation equations using the Eulerian-Eulerian (EE) multi-fluid approach. Unlike the Eulerian-Lagrangian (EL) tracking method, which computes individual particle trajectories, the EE approach treats the gas and solid phases as interpenetrating continua. This enables highly efficient evaluation of dense gas-solid flows, in which the solid phases are modeled as hypothetical fluids interacting via fluid-dynamic drag forces (Meier et al., 2011; Costa et al., 2013; Sgrott et al., 2015).

The choice of the EE framework was motivated by both physical and computational considerations. For industrial-scale cyclones with multiple interacting particle classes, the EE methodology is widely recognized as an efficient and reliable alternative to Eulerian-Lagrangian tracking, particularly when the objective is to capture macroscopic phenomena such as particle accumulation, wave formation, and collective discharge events.

The standard configuration of CYCLO-EE5 utilized in this study is hexaphasic, with one gaseous phase and five distinct solid phases (E5) characterized by different mean diameters and volume fractions. The momentum transfer at the interface between the continuous gas phase and the dispersed solid phases is governed by four-way coupling, accounting for both gas-solid and solid-solid interactions, which is essential for capturing particle accumulation and wave formations (Costa et al., 2013).

To close the RANS (Reynolds-Averaged Navier-Stokes) equations, a hybrid turbulence closure based on the standard $k-\epsilon$ model and Prandtl's mixing-length model was employed. This RANS-based approach has

been successfully validated for strongly swirling cyclone flows in previous studies by Meier and Mori (1998), Meier et al. (2011), Costa et al. (2013), and Sgrott et al. (2015).

The numerical solution is based on the finite volume method using a staggered grid arrangement. The pressure-velocity coupling is addressed by the SIMPLEC algorithm, and time integration is performed via an implicit first-order scheme to ensure numerical stability. The boundary conditions established for the simulations included a uniform velocity profile at the tangential inlet, a no-slip condition for the gas phase at the walls, and a free-slip condition for the solid phases. Continuity conditions were applied at the gas and solid outlets (Meier & Mori, 1998).

To ensure the reliability of the spatial discretization without incurring prohibitive computational costs, the grid generation parameters (i.e., the distribution of radial and axial nodes) were established strictly based on previously validated Grid Convergence Index (GCI) studies performed for the CYCLO-EE5 code on similar industrial-scale cyclonic geometries (Sgrott et al., 2015). By adopting these optimized mesh parameters, the numerical solution maintains a documented balance between high accuracy and computational efficiency, effectively mitigating discretization errors.

2.2. Modular Generator and Spark Arrester

The Modular Generator uses pine wood chips with a maximum moisture content of 50% [wet basis, WB] as fuel. The primary air entering from beneath the reciprocating grate cools the cast-iron elements of the grate. This preheated air acts on drying, volatile release, and fuel combustion. The secondary air, injected over the combustion area, is intended to contact the gases generated by combustion, reacting with them to reduce the carbon monoxide concentration (an exothermic reaction to carbon dioxide) and releasing energy as heat in the process. All gases from the Modular Generator pass through two spark arresters installed at the generator's gas outlet. Since the inlets are symmetrical, it is assumed that the flow rate at the inlet of each spark arrester is half of the total generator outlet flow. Figure 1 presents details of the Modular Generator coupled to the spark arrester, highlighting the flow symmetry at the spark arrester inlets, while Figure 2 provides the geometric details of the spark arrester.

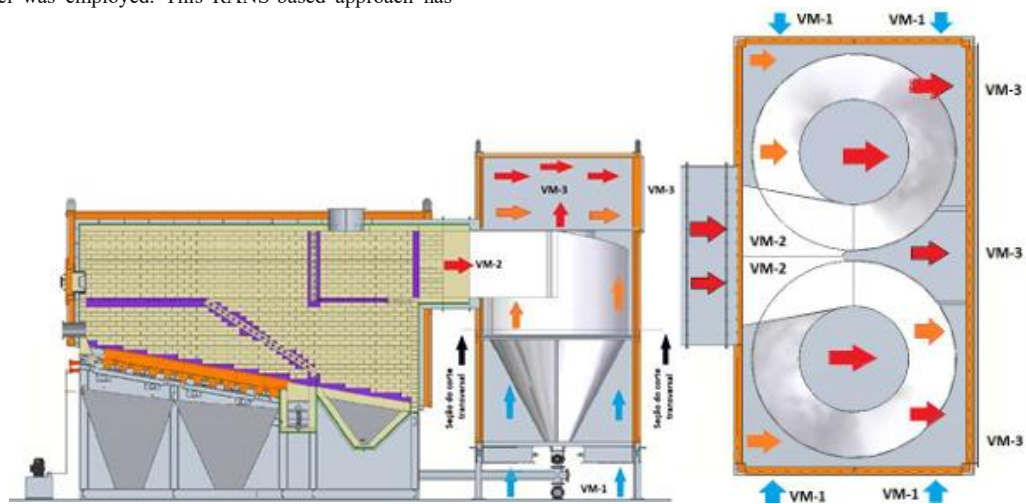


Figure 1. Schematic drawing of the Modular Generator (left) and top view of the spark arresters.

Given the objective of analyzing experimental and numerical data, the equipment's design specifications were strictly followed. Thus, based on the particle size distribution of pine wood chip ash obtained from the spark arrester's solid outlet (DI) at an industrial scale, five solid phases were defined for the code. The parameters for mean diameter (dp) and mass fraction (f) are as follows: $dp1 = 85$ mm with $f1 = 39,47\%$; $dp2 = 60$ mm with $f2 = 13,16\%$; $dp3 = 45$ mm with $f3 = 9,21\%$; $dp4 = 35$ mm

with $f4 = 22,37\%$ and $dp5 = 20$ mm with $f5 = 15,79\%$. The applied operating conditions further consider a gas mass flow rate of 20.55 kg/s, a solid density of 600 kg/m³, and a solid mass flow rate of 1.7032×10^{-4} kg/s, all at a temperature of 800°C .

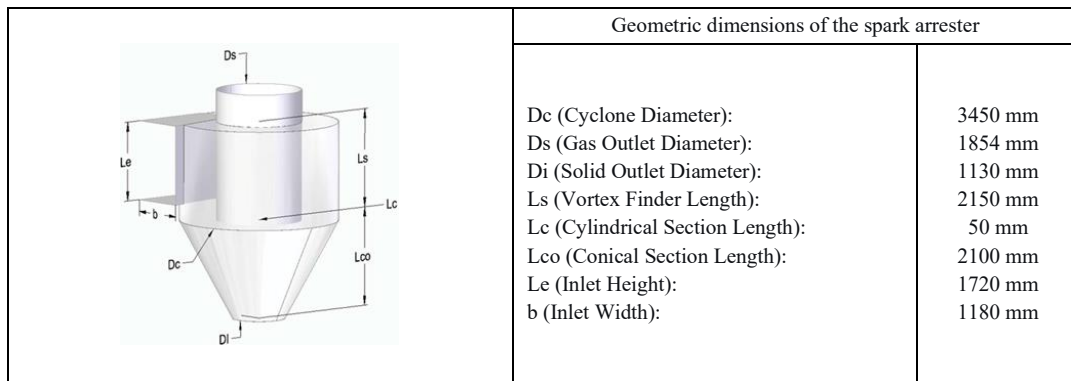


Figure 2. Geometric dimensions and details of the spark arrester.

2.3. Experimental Setup and Uncertainty Quantification

An in situ experimental investigation was conducted on a fully operational industrial spark arrester to monitor its real-time fluid-dynamic behavior and establish a quantitative baseline for numerical validation. Differential pressure measurements were continuously recorded across the equipment, with the sampling probes installed at the inlet duct and the vortex finder outlet. The data acquisition was performed using an industrial piezoresistive pressure transmitter (Ecil, model Chemist 600), which features a calibrated measurement range of -10 to 200 hPa, a resolution of 0.01 hPa, and an instrumental accuracy of $\pm 1\%$ of the full scale.

To adequately capture the frequency and amplitude of the transient pressure fluctuations, which are indicative of the intermittent particle discharge (avalanche effect), data acquisition was carried out continuously over a 205 s operational window at a sampling frequency of 1 Hz. Rather than relying on steady-state point measurements, this continuous time-series approach provided a dynamic dataset of 205 points. Given the inherent complexities of a full-scale, actively operating industrial plant, establishing steady-state conditions to perform traditional experimental triplicates was not feasible. Therefore, this continuous time-series approach was designed as a phenomenological investigation. The $\pm 1\%$ instrumental uncertainty limits provide reliability bounds for the pressure readings, ensuring that the observed macroscopic oscillatory behavior is physically consistent and effectively validating the dynamic phenomena predicted by the transient CFD model.

3. Results and Discussion

The following results present numerical and experimental analyses of an industrial-scale cyclonic spark arrester. Figure 3 shows the simulated

pressure (Figure 3a) and tangential velocity (Figure 3b) fields, which are fundamental to understanding the equipment's internal dynamics.

In Figure 3a, the formation of a low-pressure core is observed at the center of the cyclone ($r = 0$), extending from the vortex finder outlet to the base of the cone. The lowest values are concentrated in the conical region, just below the cylindrical section. In conventional cyclones, such as the Lapple and Stairmand models, this low-pressure core is typically restricted to the cylindrical region, functioning as a stabilizing element for the swirling flow. In the case of the spark arrester, however, the natural length of the vortex is not maintained, evidencing that the geometry was not designed to reproduce the phenomenological conditions typical of high-efficiency cyclones.

Figure 3b presents the tangential velocity field. Unlike the central region ($r = 0$), where the tangential velocity is zero, the intense rotational flow is concentrated between $r = 0.25$ and $r = 0.70$, extending along the entire axial axis to the base of the cone. In standard cyclones, this high-velocity field is more compact and located near the cylindrical region. In the spark arrester, however, the vortex shows significant elongation in the axial direction, indicating that if the cone were longer, the rotation would tend to advance even further in that direction. This behavior confirms that the equipment has an axial dimension smaller than the ideal, compromising the formation and stability of the vortex.

From a practical standpoint, these observations have direct implications for collection efficiency and the risk of incandescent particle emission. The current geometry favors flow instability and intermittent collection regimes, which contribute to the re-entrainment of solid material toward the outlet. This result corroborates the hypothesis that the oscillatory dynamics of the spark arrester may be a determining factor in spark emission and, therefore, in the operational safety of grain dryers.

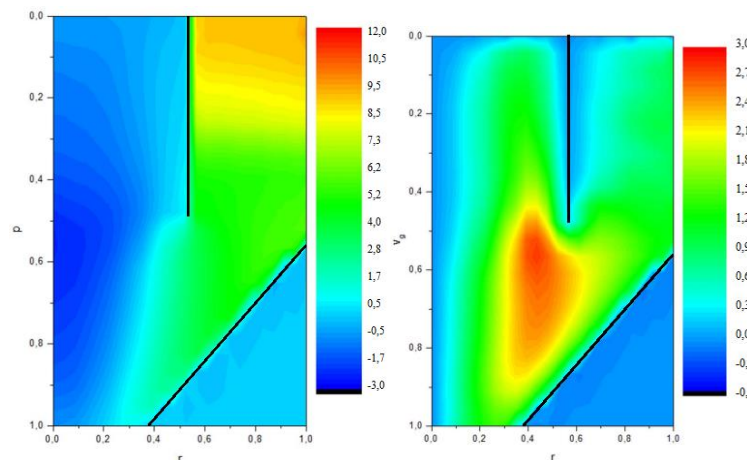


Figure 3. Pressure profile map and tangential velocity across the spark arrester diameter.

Figure 4a presents the numerical results of the separation efficiency for the cyclonic spark arrester, considering both the bottom outlet (overflow) and the top outlet (vortex finder). It is observed that only after approximately 25,000 s of simulation do the efficiency dynamics reach a

stable oscillatory regime, a behavior like that observed for the pressure drop (Figure 4b).

The efficiency at the vortex finder ranged from 70.5% to 72%, while at the overflow, it oscillated between 64% and 72.5%. This range of

variation demonstrates that the system does not operate under a continuous collection regime but rather experiences intermittent accumulation and discharge of particulate matter. During accumulation periods, the collection efficiency remains reduced; however, when a sudden discharge of this material occurs—characterized by the so-called avalanche effect—the efficiency reaches a momentary maximum.

From an applied standpoint, this oscillatory dynamic implies a higher risk of re-entrainment of incandescent particles into the outlet flow, which is a critical factor for the safety of grain dryers.

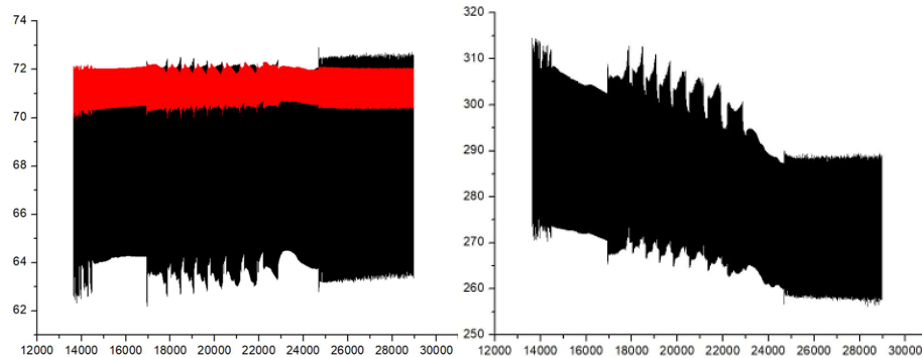


Figure 4. Separation efficiency (%) (left) and pressure drop (mmH₂O) (right) over a wide time range (s).

Figure 5 presents the dynamics of the volume fractions for each particle size class considered in this numerical study ($dp_1 = 85 \mu\text{m}$, $dp_2 = 60 \mu\text{m}$, $dp_3 = 45 \mu\text{m}$, $dp_4 = 35 \mu\text{m}$, and $dp_5 = 20 \mu\text{m}$, respectively, from left to right).

The dynamic behavior of these distinct particle classes can be analytically understood through the Stokes number (St), defined as the ratio of the

particle relaxation time to the characteristic time of the fluid flow. For the larger particles (dp_1 and dp_2), the higher St values indicate that inertial forces dominate. These particles are readily centrifuged towards the walls, where they accumulate and form dense, high-concentration waves (particle ropes) near the base of the vortex finder (Hoffmann & Stein, 2008).

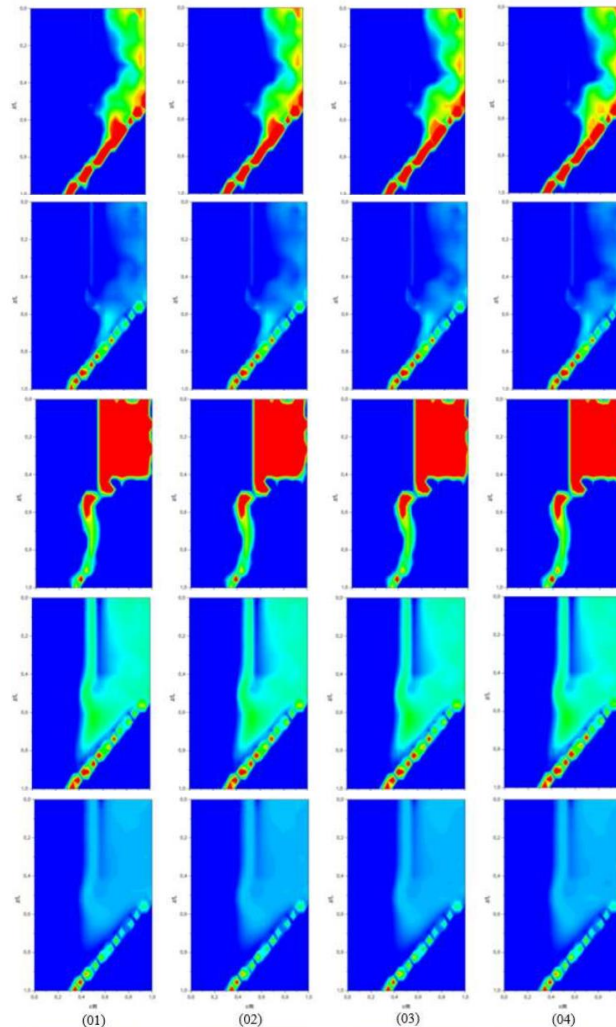


Figure 5. Solid volume fraction for dp_1 , dp_2 , dp_3 , dp_4 , and dp_5 , respectively.

However, as the particle diameter decreases (dp_4 and dp_5), the St number significantly reduces ($St \ll 1$), meaning the particle's aerodynamic response closely follows the turbulent fluid streamlines. Consequently,

these finer fractions do not possess sufficient inertia to penetrate the boundary layer at the walls and are instead caught in the highly turbulent shear zones and flow reversal regions.

In the case of dp2, wave growth toward the vortex finder is noted, forming a distinct "tongue" of particulate matter. For dp3, the advancement of particles toward the vortex finder is even more pronounced, accompanied by material accumulation in the annular region between the cylinder and the vortex finder, where discharge waves are formed.

As for dp4 and dp5, a continuous flow reversal is observed, extending from the outlet of the cylindrical section to the reversal region at the base of the cone. This indicates that larger particles (dp1 and dp2) undergo re-entrainment mainly at the outlet of the cylindrical section, where the upward flow resulting from the reversal at the cone base meets the downward flow from the tangential inlet. On the other hand, the smaller particles (dp4 and dp5), due to their low Stokes number, are more susceptible to re-entrainment, both by the shearing between downward and upward flows and by the effect of the reversal itself.

These observations, combined with the pressure drop results, provide evidence of an intermittent collection regime characterized by accumulation and discharge cycles. This behavior compromises the spark arrester's retention efficiency and increases the probability of emitting unburned particles into the outlet flow, posing an additional risk to the safety of grain dryers.

The analysis of a reduced 5 s time window (Figure 6) more clearly highlights the simultaneous oscillations in separation efficiency at both the vortex finder and the overflow, as well as the pressure drop in the spark arrester. It is observed that all three variables exhibit the same

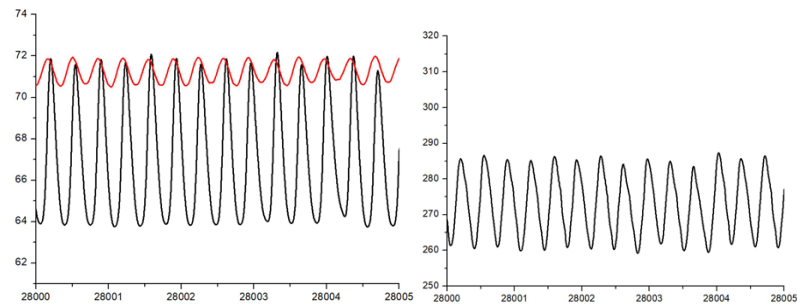


Figure 6. Separation efficiency (%) (left) and pressure drop (mmH₂O) (right) for 5 s of simulation.

Experimental pressure drop data were obtained during continuous operation for 205 s, with data acquired every second (Figure 7). The results highlight pressure oscillations characteristic of particle avalanches within the cyclone. Although the amplitudes and frequencies of these peaks do not exactly coincide with the numerically predicted values, the same trend of periodic oscillations is observed, qualitatively confirming intermittent material discharges.

This behavior is attributed to the entrainment of unburned particles, which find a preferential path toward the spark arrester outlet. The experimental validation, albeit qualitative, demonstrates that the CYCLO-EE5 code can realistically predict the oscillatory phenomena associated with discontinuous discharge, which has not been previously described in the literature for this type of equipment. From an applied standpoint, these results reinforce the need to consider avalanche dynamics in the design and operation of spark arresters, as avalanche dynamics are directly associated with the risk of spark emission in grain dryers.

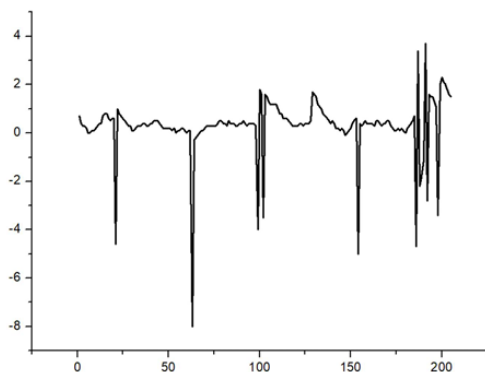


Figure 7. Experimental pressure drops (mmH₂O) for 205 s.

In summary, the results obtained in this study reveal that the spark arrester operates under an unstable flow regime, characterized by an elongated low-pressure core, tangential high-velocity fields along the axial direction, and

oscillation frequency of approximately 2.8 Hz (corresponding to 14 distinct peaks within the 5s window). This quantifies a highly cyclic phenomenon intrinsic to the flow. Recent reviews on cyclonic fluid dynamics highlight that the internal airflow is not perfectly steady; rather, it fluctuates in a predictable, repeating pattern driven by hydrodynamic instabilities, such as the processing vortex core (PVC) (Aylı & Kocak, 2025). Furthermore, advanced multiphase flow models demonstrate that such periodic instabilities are directly associated with the formation and accumulation of dense solid structure, often termed "particle ropes" or "particle banded flow", along the cyclone walls (Hoffmann & Stein, 2008; Li et al., 2023). The formation of these dense bands alters local shear stresses and fluid velocities. When these accumulated structures reach regions of high shear or flow reversal, they collapse and are intermittently discharged or re-entrained into the bulk, directly causing the observed simultaneous pressure fluctuations and efficiency drops. This confirms that the numerically predicted "avalanche effect" is a macroscopic behavior of these transient multiphase flow instabilities.

From a practical standpoint, this periodic oscillation confirms the occurrence of unstable collection regimes associated with the re-entrainment of unburned particles toward the spark arrester outlet. Such a result reinforces the relevance of the numerical model not only as a predictive tool but also as support for redesigning more efficient and safer geometries for agro-industrial applications.

intermittent cycles of particle accumulation and discharge. The numerical analyses showed that these oscillations directly affect collection efficiency and pressure drop, thereby characterizing the phenomenon of particulate material avalanche, which was subsequently qualitatively confirmed by experimental pressure data. The dynamics observed across different particle-size ranges showed that both larger particles, due to re-entrainment at the cylindrical outlet, and smaller particles, due to shear effects and flow reversal, contribute to the instability process. From a practical standpoint, this instability is associated with the re-entrainment of potentially incendiary unburned particles, thereby increasing the risk of safety failures in grain dryers. Thus, the results presented here not only validate the predictive capacity of the CYCLO-EE5 code but also offer contributions to the understanding of spark arrester fluid dynamics, establishing a basis for future improvements in the design and operation of this equipment in the agro-industry.

From a practical and design perspective, mitigating the avalanche effect and the subsequent re-entrainment of incendiary particles requires geometric optimization. The numerical pressure and velocity fields (Figure 3) demonstrated that the spark arrester's vortex elongates excessively, reaching the very bottom of the conical section. Based on classical cyclone optimization principles, increasing the length of the conical section (L_{co}) could prevent the highly turbulent inner vortex core from interacting directly with the collected dust bed. By establishing a physical or aerodynamic barrier at the flow reversal point, the structural integrity of the descending particle ropes could be maintained, thereby dampening the 2.8 Hz pressure oscillations and stabilizing the overall spark retention efficiency.

4. Conclusions

The integrated application of advanced numerical simulation and in situ experimental analysis enabled the identification of intermittent accumulation and discharge of particulate matter within cyclonic spark arresters. This transient behavior was numerically characterized by simultaneous oscillations in collection efficiency and pressure drop at

approximately 2.8 Hz, associated with the formation and collapse of dense particle ropes (the avalanche phenomenon), and was phenomenologically confirmed by continuous industrial-scale measurements.

The results demonstrated that the current equipment geometry favors unstable flow regimes. Dictated by their respective Stokes numbers, larger particles accumulate and undergo re-entrainment at the cylindrical outlet, while smaller, low-inertia particles are caught by highly turbulent shear zones and flow reversal. This dynamic severely compromises retention efficiency and elevates the risk of emitting potentially incendiary unburned particles toward downstream processes.

The novelty of this study lies in demonstrating that spark arrester performance cannot be accurately predicted solely by classical steady-state empirical models of average efficiency; it must account for the highly transient and oscillatory nature of particle collection. Consequently, this finding establishes that specific geometric modifications are required to damp these periodic instabilities and stabilize the vortex core.

From an applied standpoint, the evidence presented here directly contributes to the safety and sustainability of the agribusiness sector, providing robust technical support for the geometric redesign and operational optimization of spark arresters, ultimately mitigating fire risks in grain-drying systems.

Acknowledgments

The authors would like to acknowledge the University of Blumenau (FURB) for its institutional support and infrastructure.

Declaration of Generative AI and AI-assisted technologies in the writing process

During the preparation of this work, the authors used Gemini to perform technical translation and refine the English of the manuscript. After using this tool, the authors reviewed and edited the content as needed.

References

- Alexander, R. M. K. (1949). Fundamentals of cyclone design and operation. *Proceedings of the Institution of Mining and Metallurgy*, 152–153, 203–228.
- Aylil, E., & Kocak, E. (2025). A comprehensive review of cyclone separator technology. *The Canadian Journal of Chemical Engineering*, 103, 2751–2789.
- Chen, T., Van Caneghem, J., Degrève, J., Verplaetsen, F., Berghmans, J., & Vanierschot, M. (2022). A numerical model for the calculation of the minimum ignition energy of pure and mixture dust clouds. *Process Safety and Environmental Protection*, 164, 271–282.
- Companhia Nacional de Abastecimento. (2025, August 14). *Grain harvest 2024/25 is estimated at 345.2 million tons, with record production of corn and soybeans*. Ministry of Agrarian Development and Family Agriculture. <https://www.gov.br/conab/pt-br/assuntos/noticias/safra-de-graos-2024-25-e-estimada-em-345-2-milhoes-de-toneladas-com-recorde-na-producao-de-milho-e-soja>
- Costa, K. K., Sgrott Jr., O. L., Decker, R. K., Reinehr, E. L., Martignoni, W. P., & Meier, H. F. (2013). Effects of phases' numbers and solid–solid interactions on the numerical simulations of cyclones. *Brazilian Journal of Chemical Engineering*, 32, 1567–1572.
- Ding, J., Qi, C., Yan, X., Lv, X., Zhang, S., Liang, H., Fan, T., & Yu, J. (2024). Effect of airflow velocity on flame propagation and pressure of starch dust explosion in a pneumatic conveying environment. *Powder Technology*, 433, Article 119147
- Eckhoff, R. K., & Li, G. (2021). Industrial dust explosions: A brief review. *Applied Sciences*, 11(4), 1669.
- Hoffmann, A. C., & Stein, L. E. (2008). *Gas cyclones and swirl tubes: Principles, design and operation*. Springer.
- Huang, C., Wang, S., Chu, Y., Chen, Y., Chen, X., Liu, L., & Zhang, H. (2022). Comprehensive investigations on the explosion suppression of biomass fuels: Starch as a representative. *Fuel*, 315, Article 123276.
- Li, Q., Cheng, T., Li, Q., Liu, J., Liang, Y., Li, J., Jiang, X., Wang, H., & Fu, P. (2023). Particle high-speed self-rotation in cyclones with different diameters and application in catalyst deoiling. *Journal of Cleaner Production*, 423, Article 138681.
- Meier, H. F., & Mori, M. (1998). Gas–solid flow in cyclones: The Eulerian–Eulerian approach. *Computers & Chemical Engineering*, 22(Suppl.), S641–S644.
- Meier, H. F., Vegini, A. A., & Mori, M. (2011). Four-phase Eulerian–Eulerian model for prediction of multiphase flow in cyclones. *The Journal of Computational Multiphase Flows*, 3(2), 92–105.
- Sgrott Jr., O. L., Noriler, D., Wiggers, V. R., & Meier, H. F. (2015). Cyclone optimization by COMPLEX method and CFD simulation. *Powder Technology*, 277, 11–21.
- Sulaiman, S. Z., Mohd Mokhtar, K., Wan Sulaiman, W. Z., & Semawi, N. H. (2024). Flame propagation and explosion characteristics of food-based dust as a function of dust concentration. *Process Safety Progress*, 43(3), 579–586.
- Tascón, A., Ramírez-Gómez, Á., & Aguado, P. J. (2016). Dust explosions in an experimental test silo: Influence of length/diameter ratio on vent area sizes. *Biosystems Engineering*, 148, 18–33.
- Tian, C., Yang, Z., & Zhang, L. (2025). A review of grain dust explosions: Prevention and control. *Results in Engineering*, 26, Article 105483.
- Zarpellon, L. E., Nascimento, D. G., Silva Neto, J. S., Castro, K. A., Pereira Junior, M. F., & Silva, T. V. (2025). Análise de incêndios em secadores de grãos: Investigação de causas e estratégias de prevenção para retroalimentação de normas de segurança. *Revista FLAMMAE*, 11(34).
- Zhang, J., Li, C., Li, G., Du, Z., Bao, S., Zhang, Z., & Yuan, C. (2024). Effect of large particle mixing on cloud ignition and explosion of fine rice husk. *Process Safety and Environmental Protection*, 191, 304–314.
- Zhao, Y., & Ambrose, R. P. K. (2019). Modeling dust dispersion and suspension pattern under turbulence. *Journal of Loss Prevention in the Process Industries*, 62, Article 103934.
- Zhao, Y., & Ambrose, R. P. K. (2022). Predicting continuous dispersion and deposition of explosive dust in confined spaces using a discrete phase model. *Powder Technology*, 408, Article 117704.